JACS
JOURNAL OF THE AMERICAN CHEMICAL SOCIETY
Article
pubs.acs.org/JACS

One-Point Binding Ligands for Asymmetric Gold Catalysis: Phosphoramidites with a TADDOL-Related but Acyclic Backbone

Henrik Teller, Matthieu Corbet, Luca Mantilli, Gopinadhanpillai Gopakumar, Richard Goddard, Walter Thiel, and Alois Fürstner*

Max-Planck-Institut für Kohlenforschung, D-45470 Mülheim/Ruhr, Germany

Supporting Information

ABSTRACT: Readily available phosphoramidites incorporating TADDOL-related diols with an acyclic backbone turned out to be excellent ligands for asymmetric gold catalysis, allowing a number of mechanistically different transformations to be performed with good to outstanding enantioselectivities. This includes [2 + 2] and [4 + 2] cycloadditions of ene-allenes, cycloisomerizations of enynes, hydroarylation reactions with formation of indolines, as well as intramolecular hydroaminations and hydroalkoxylations of allenes. Their preparative relevance is underscored by an application to an efficient synthesis of the antidepressive drug candidate (−)-GSK 1360707. The distinctive design element of the new ligands is their acyclic dimethyl ether backbone in lieu of the (isopropylidene) acetal moiety characteristic for traditional TADDOL's. Crystallographic data in combination with computational studies allow the efficiency of the gold complexes endowed with such one-point binding ligands to be rationalized.

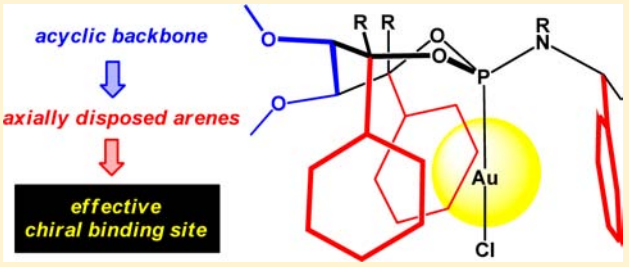

INTRODUCTION

Transition metal-catalyzed cycloisomerization reactions of 1,*n*-enynes and related compounds allow high levels of molecular complexity to be attained in a fully atom economical fashion from fairly simple unsaturated substrates.[1] Following the pioneering work on Alder-ene reactions,[2] the systematic use of carbophilic Lewis acids added an additional dimension to this timely field of catalysis research. Platinum took the lead,[3,4] closely followed by gold catalysis, which reached tremendous popularity in recent years.[5]

To take full advantage of the preparative potential of such transformations, it is mandatory to develop efficient asymmetric variants.[6,7] Gold catalysis, however, poses particular challenges in this regard: since Au(+1) favors a linear-dicoordination geometry, the substrate to be activated and the chiral ancillary ligand L* are positioned *trans* to each other, sandwiching the very bulky metal center (Chart 1).[5,6] As only one coordination site is available for L* and chelation therefore excluded, the rotation about the L*−Au bond remains, a priori, unrestricted. An additional complication arises from the fact that gold-catalyzed reactions are generally believed to be outer-sphere processes, in which the nucleophile does not enter the first coordination sphere of the metal; rather, it attacks the π-system from the back side and hence at maximum distance from the inducing ligand L*, while the gold template slips away along the π-bond when the nucleophile approaches.[8]

Three major strategies to tackle these exigent problems have emerged so far.[6] The first concept outsources the duty of creating a chiral binding pocket from the cationic metal template to the escorting anion. If a sufficiently tight ion pair is formed in solution, high asymmetric induction can be achieved, as demonstrated by some intramolecular hydroamination and hydroalkoxylation reactions of allenes controlled by bulky chiral phosphonates of type **1** (Chart 1).[9−11]

Chart 1. Asymmetric Gold Catalysis: Established Design Concepts Based on Chiral Counterions or on Chiral Dinuclear Gold−Phosphine Complexes

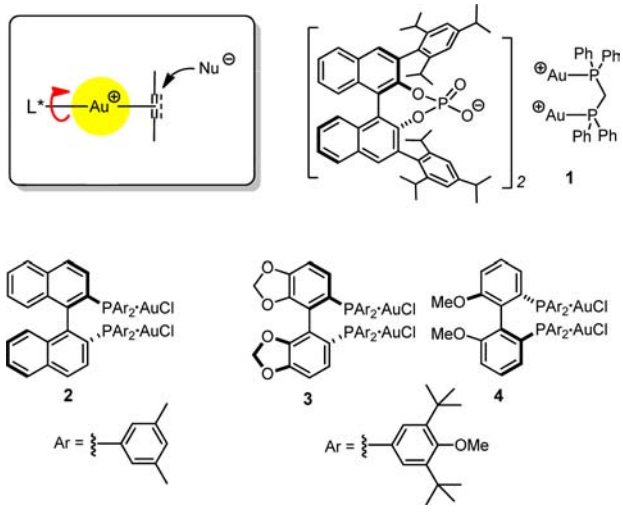

Received: April 16, 2012
Published: August 27, 2012

   dx.doi.org/10.1021/ja303641p | J. Am. Chem. Soc. 2012, 134, 15331−15342

The second and more common approach relies on chiral bisphosphine ligands of proven versatility, frequently axially chiral ones of the BINAP, SEGPHOS, or BIPHEP types.[12,13] As chelation is precluded, however, any such bisphosphine necessarily picks up 2 equiv of Au(+1) to give the corresponding dinuclear complexes such as **2**–**4** (Chart 1). Provided that their P-atoms carry large substituents, such species served a variety of gold-catalyzed transformations well. Whether or not aurophilic contacts between the individual gold centers assist the asymmetric induction remains to be fully elucidated.[14] Similar arguments hold true for the small number of chiral bis-carbene gold complexes used to date.[15]

The third successful approach relies on *monodentate* chiral ligands L*. Although an early attempt to use the BINOL-derived phosphoramidite **5** in the alkoxycyclization of 1,6-enynes had essentially met with failure,[12b] three groups, including our own, managed to overcome this discouraging start. Specifically, it was shown that bulky groups attached to the 3,3′-positions of the BINOL subunit, as borne out in ligands **6**–**8** (Chart 2), can lead to largely improved results in various gold-catalyzed transformations.[16−20]

Chart 2. BINOL-Derived Phosphoramidite Ligands for Asymmetric Gold Catalysis

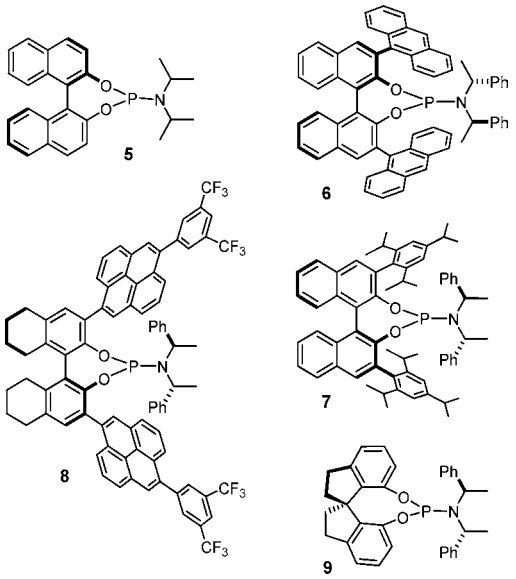

These encouraging results demonstrate that the challenges of asymmetric gold catalysis can ultimately be met even with proper one-point-binding ligands. Yet, a systematic structural editing of ligands such as **6**–**9** is cumbersome, the size of the required lateral substituents unappealing, and the molecular weights of the derived gold complexes rather high. Similar arguments pertain to the massive dinuclear gold complexes such as **2**–**4**, which are based upon expensive ligand scaffolds that are also rather difficult to modify.

These issues let us embark on a search for alternative ligand architectures, which, ideally, should be small, cheap, tunable, yet highly effective. Although the phosphoramidites with a TADDOL-related but acyclic backbone presented below do not meet all of these criteria equally well, they impose remarkable levels of asymmetric induction onto a variety of mechanistically distinct gold-catalyzed transformations and therefore constitute a serious alternative.[18] Structural and computational data allow their effectiveness to be rationalized, whereas an application to the synthesis of a drug candidate under clinical development underscores their practical relevance.

RESULTS AND DISCUSSION

Ligand Design. Apprehensive that the free rotation of the chiral monodentate ligand L* about the L*–Au bond is a critical issue, our design was originally predicated on symmetry considerations. Specifically, it was reasoned that a C_3-symmetric ligand environment might craft a chiral binding pocket about the metal that is invariant to rotation. To test this hypothesis, we chose the gold-catalyzed [2 + 2] cycloaddition of ene-allene **11**. This transformation is a rigorous benchmark, because it has already been accomplished with no less than 95% ee by using the dinuclear SEGPHOS-based gold complex **3**.[21] Moreover, this reaction is known to be sensitive to the electronic nature of the ligand bound to gold.[22]

Among the small set of ligands considered in the first place, our screening identified TADDOL-derived phosphoramidites as promising hits. For example, the parent complex **10a** furnished product **12** in excellent yield and 84% ee.[23−25] However, neither steric nor electronic variations of the lateral arenes nor replacement of bis[(*R*)-1-phenethyl]amine by other amine constituents lead to any significant improvement (Scheme 1).[18] Changing the solvent, counterion, and/or temperature was to no avail either.

Scheme 1. Initial Screening of TADDOL-Derived Phosphoramidite–Gold Complexes in a [2 + 2] Cycloaddition

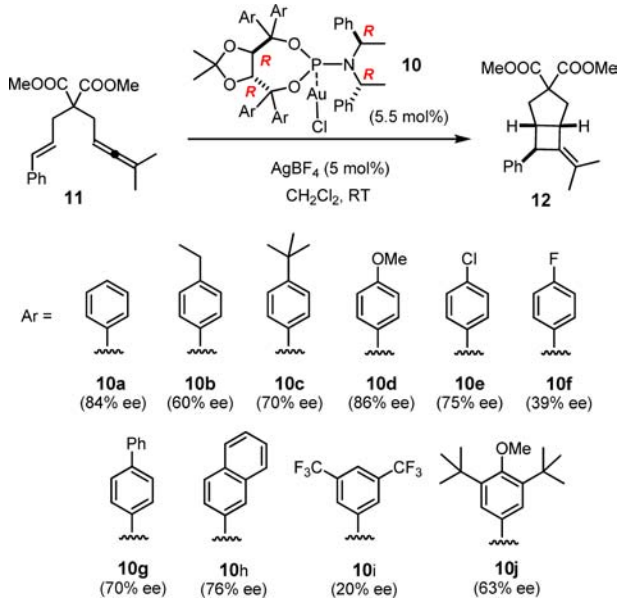

In contrast to these unsuccessful attempts at an empirical ligand optimization, a rational approach was ultimately more rewarding. Hand-held models of complex **10a** had suggested that three of the peripheral phenyl rings might form a conic cavity of approximate C_3 symmetry about the gold center.[26] While this notion was confirmed by the X-ray structure of this complex,[18] a more detailed inspection showed that the distances between the metal and the phenyl rings in question are not uniformly close; one of the two relevant phenyl

dx.doi.org/10.1021/ja303641p | J. Am. Chem. Soc. 2012, 134, 15331−15342

substituents on the TADDOL is notably bent away from the gold atom. Therefore it seemed reasonable to refine the ligand design such that all three decisive aryl rings are brought into a fully upright orientation and hence into close proximity to the Au center.

To this end, it was necessary to adjust the puckering of the phosphoramidite's basal ring. Whereas substitution of the isopropylidene group by more bulky acetal moieties (cf. **13** and **14**) led to a considerable erosion of the optical purity, the formal replacement of the acetal altogether by a dimethyl ether motif, as borne out in complex **15a**, substantially increased the ee of product **12** to 94% (Chart 3). To the best of our knowledge, such TADDOL-related compounds with an acyclic backbone had no notable history in asymmetric catalysis prior to this work.[27]

Chart 3. Impact of the TADDOL Backbone on the Asymmetric Induction upon Formation of Cycloadduct 12 and the Structure of Complex 15a in the Solid State[18]

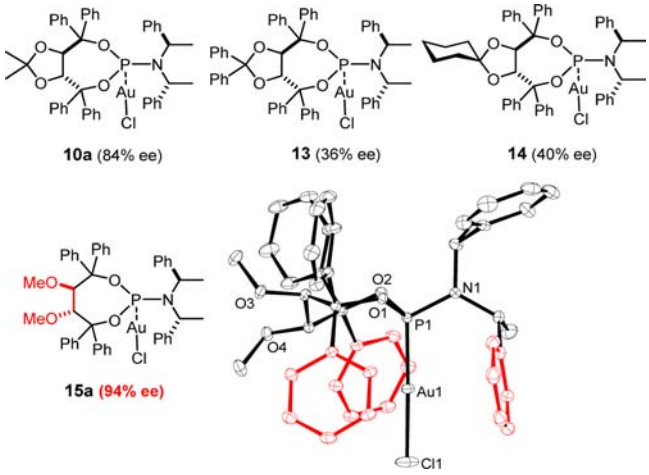

The structure of the fully air-stable gold complex **15a** in the solid state features a regular and very tight conic binding pocket of effective C_3 symmetry.[18] All three phenyl rings forming the walls of this cavity are strictly axially disposed on the basal seven-membered ring. Secondary interactions between the arene-π-clouds and the gold center seem to stabilize the chiral binding site.[28] The side view depicted in Chart 3 is particularly instructive: it shows that the phenyl rings reach over the gold atom, but not by much. Actually, any π-system bound to the metal after ionization of the Au–Cl bond will reside close to the cavity's outer rim. Immersing the substrate deeper into the pocket should result in more effective chirality transfer. The projection in Chart 3 suggests that either an appropriate substituent at the *para*-position of the phenyl groups or annulation of a second ring should craft such an extended binding site, which might result in effective control over an ensuing outer-sphere reaction. The structure of complex **15b** with strategically placed *tert*-butyl groups on the periphery is in fact suggestive (Figure 1). The same holds true for the 2-naphthyl variants **15c,d**, which are discussed in more detail below. It is important to note already at this point, however, that the effective C_3 symmetry of these precatalysts turns into a C_1 symmetric environment upon substrate binding, as indicated by the computational studies outlined below. In any case, these novel gold complexes are air-stable and therefore easy to use,

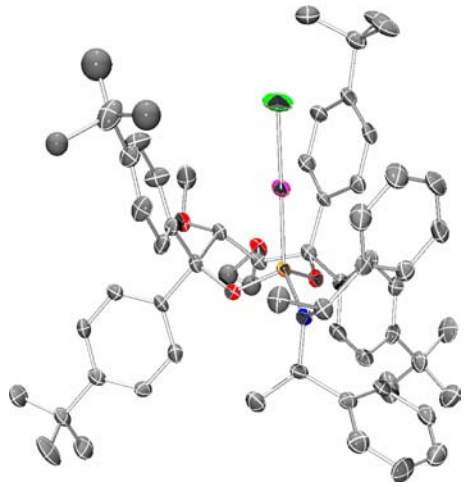

Figure 1. Structure of complex **15b** in the solid state.

and the required ligands are readily prepared in either enantiomeric form on a multigram scale as shown in Scheme 2.

Scheme 2. Preparation of Phosphoramidite–Gold Complexes with a TADDOL-Related but Acyclic Backbone and Prototype Examples of Either Enantiomeric Series[a]

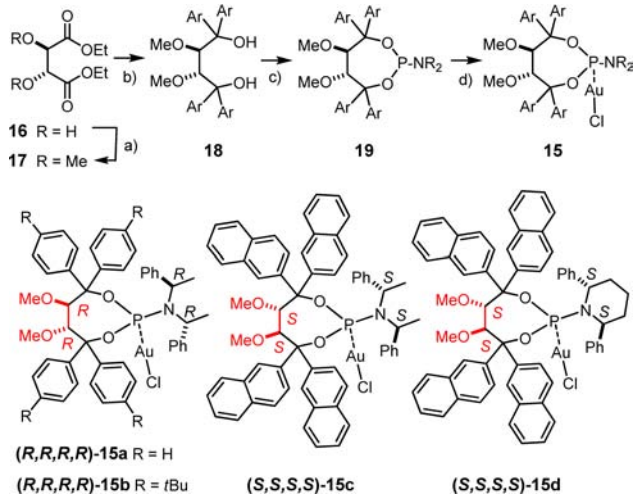

[a]Reagents and conditions: (a) NaH, dimethyl sulfate, Et_2O, 0 °C → RT, quant.; (b) ArMgBr (5 equiv), THF, 0 °C → RT, 57% (Ar = Ph), 67% (Ar = tBuC$_6$H$_4$–); or 2-bromonaphthaline, nBuLi, THF, −78 °C, 58% (Ar = 2-naphthyl); (c) (i) PCl_3, Et_3N, toluene (0.02 M), MS 4 Å, 0 °C → 60 °C, (ii) R_2NH, nBuLi, THF, −78 °C → RT, 58% (Ar = Ph), 67% (Ar = tBuC$_6$H$_4$–); (d) $NaAuCl_4 \cdot 2H_2O$, 2,2′-thiodiethanol, $CHCl_3/H_2O$ (1:5), 99% (**15a**), 95% (**15b**), 45% (**15c**, over two steps), 51% (**15d**, over two steps).

[2 + 2] and [4 + 2] Cycloadditions. In keeping with this structural information, complexes of type **15** were found to excel in the [2 + 2] cycloaddition of ene-allenes. Whereas the originally used complex **10a** based on a traditional TADDOL-subunit had given product **12** with 84% ee (Scheme 1), its acyclic cousin **15a** furnished this compound in 94% ee. Virtually perfect optical purity (≥99% ee) was secured with the extended variant **15b** carrying *tert*-butyl groups at the *para*-position. This outcome is noteworthy since any *para*-substituent, when attached to phosphoramidites comprising a traditional TADDOL subunit, had been counterproductive (see **10b–g**,

dx.doi.org/10.1021/ja303641p | J. Am. Chem. Soc. 2012, 134, 15331–15342

Scheme 1). Additional information is contained in Table S-1 (Supporting Information), which shows that complexes **15a,b** outperform a variety of (simple as well as rather sophisticated) gold complexes containing BINOL-derived phosphoramidite ligands. The result obtained with **15b** favorably compares even with the very best literature report that had used the elaborate dinuclear SEGPHOS-derived complex **3** (95% ee).[21]

The exceptional level of asymmetric induction imparted by complex **15b** on this type of [2 + 2] cycloaddition was maintained throughout a set of representative examples (Chart 4). This includes modifications at the ester, the arene, and the

Chart 4. Asymmetric [2 + 2] Cycloadditions of Ene-Allenes Catalyzed by Complex 15b[a]

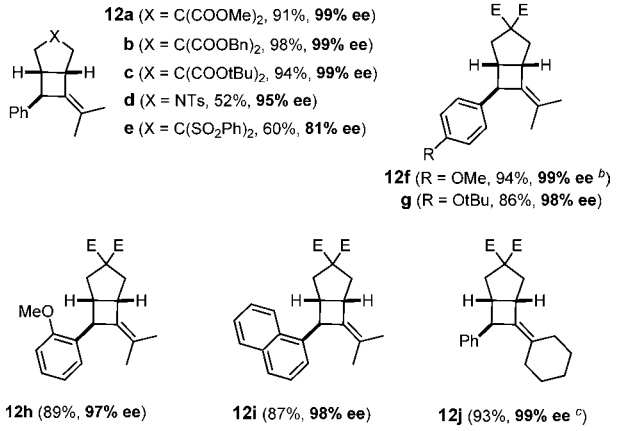

[a]All reactions were preformed with **15b** (5.5 mol %), $AgBF_4$ (5 mol %) in CH_2Cl_2 at 0 °C, unless stated otherwise. [b]Contains 6.7% of an unidentified isomer (HPLC). [c]Atambient temperature; E = COOMe.

allene sites; even the *N*-tosyl derivative **12d** was obtained with 95% ee, whereas the binuclear SEGPHOS–gold complex **3** delivered this compound with modest 54% ee.[21] Since we were able to grow crystals of this particular product, its previously unknown absolute configuration could be rigorously determined by X-ray diffraction (see the SI); all other products were assigned by analogy. Only the bis-sulfone derivative **12e** was formed with a slightly lower ee of 81% for reasons that are not entirely clear.

The new catalysts also bear comparison with the attractive *spiro*-bisindane-derived phosphoramidite **9** recently disclosed in the literature (Chart 2).[19b] The derived gold complex was reported to work well for the *N*-tosyl- and bissulfone derivatives **12d** (94% ee) and **12e** (85% ee), but gave a disappointing 14% ee in the malonate case **12a**. We hence conclude that complexes of type **15** are the currently most effective and general catalysts for transformations of this type.

Complex **15b** also gave respectable results in formal [4 + 2] cycloadditions of diene-allenes, as witnessed by the examples shown in Scheme 3.[29] Once again, the ligands with the acyclic backbone performed better than their relatives comprising a traditional TADDOL subunit (see Table S-2, SI). The comparison also shows that **15b** is a serious alternative to, in part, quite elaborate BINOL-based systems previously used,[16,19a] given the ease of synthesis and stability of this particular complex.

Enyne Cycloisomerizations. The cycloisomerization of 1,6-enynes of type **22** marks one of the beginnings of contemporary π-acid catalysis,[3,4] but the development of effective asymmetric variants turned out to be particularly

Scheme 3. Asymmetric [4 + 2] Cycloadditions of Ene-Dienes Catalyzed by 15b[a]

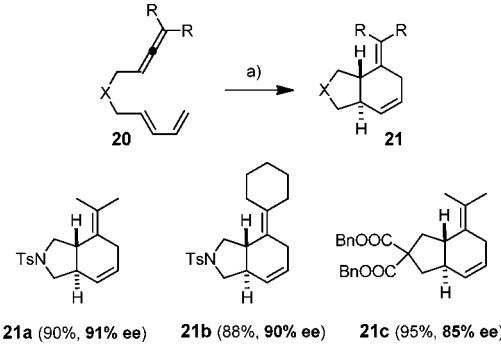

[a]Reagents and cnditions: (a) **15b** (5.5 mol %), $AgBF_4$ (5 mol %), CH_2Cl_2, 0 °C.

difficult. The standards in the field are currently set by elaborate cyclometalated Pt(+2)-complexes such as **24** endowed with P-phenyl-BINEPINE ligands.[30] Appreciable levels of enantioselectivity were also attained in select cases with the dinuclear BIPHEP-based gold complex **4**, but the chemical yields were often low.[13] The representative examples shown in Scheme 4 illustrate this situation. Chiral iridium or rhodium catalysts are also effective for certain substitution patterns (see below).[11,31]

Scheme 4. Benchmarks in the Field of Platinum- or Gold-Catalyzed Asymmetric Enyne-Cycloisomerization[13,30]

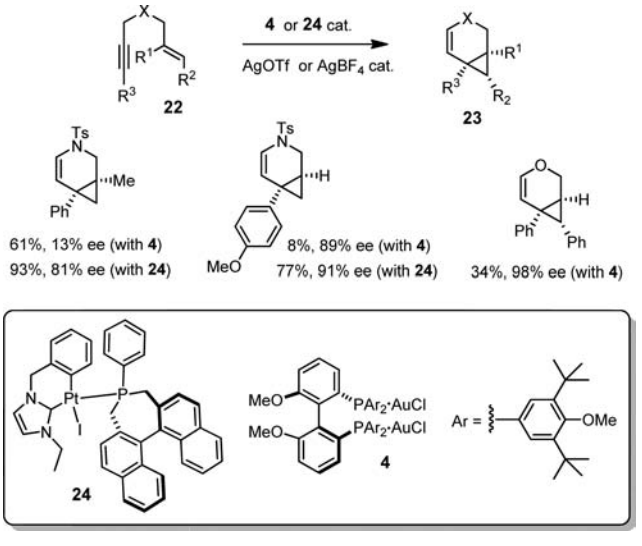

We were therefore keen to see how the new phosphoramidites epitomized by a TADDOL-related motif with an acyclic backbone perform in such transformations. It was the 2-naphthyl variant **15c** that gave the best results. Remarkable enantioselectivities as well as good to excellent yields were recorded, provided that the reactions were performed in toluene as the solvent (Chart 5). Gratifyingly, the outcome was largely independent of the chosen N-protecting group as well as of the substitution pattern of the alkene moiety. Moreover, the absolute configuration of product **23h** bearing a *p*-bromo substituent was determined by X-ray diffraction as (*R*,*R*) (see the SI); all other products were assigned by analogy.

The structure of the decisive precatalyst **15c** in the solid state (Figure 2) is distinguished by a highly regular binding site

dx.doi.org/10.1021/ja303641p | J. Am. Chem. Soc. 2012, 134, 15331−15342

Chart 5. Products of Asymmetric Cycloisomerization of N-Tethered Enynes of Type 22 (X = NR) and the Strcture of 23h in the Solid State, Which Establishes the Absolute Configuration

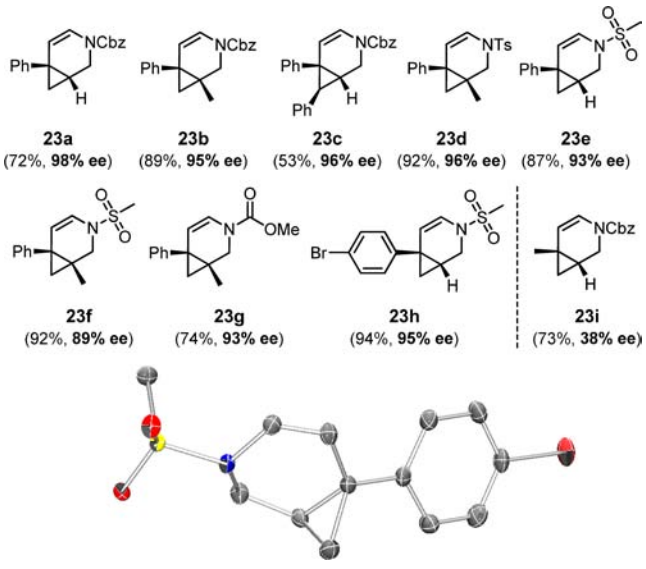

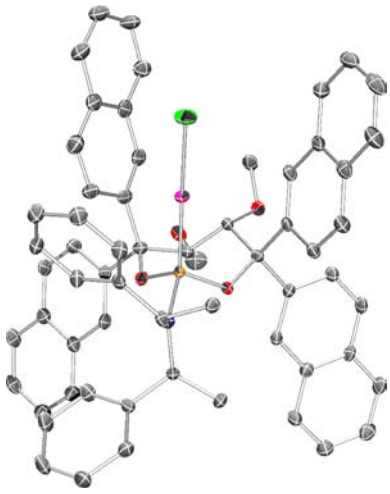

Figure 2. Structure of complex **15c** in the solid state.

formed by the ligand's aryl periphery. The chiral cavity clearly extends beyond the gold atom; its tightness transpires from the short distances between the central metal and the edges of the aromatic rings, which are tilted toward the metal.[28] These secondary interactions are thought to stabilize the catalyst and may hence play a supportive role for the asymmetric reaction.

What is less intuitive though is the fact that the enyne substrates **22** must have an aryl ring on their alkyne unit to procure high ee's (R^3 = aryl). In contrast, the corresponding enyne **22i** (X = NCbz, $R^1 = R^2 = H$, R^3 = Me) with a methyl cap gave product **23i** in good yield but with only 38% ee. The exact same innate correlation between the nature of the alkyne terminus R^3 and the enantioselectivity was noticed in the O-tethered series (vide infra). The computational study outlined below in more detail suggests that the similar steric demand of the incipient cyclopropyl ring and the methyl group is to be blamed for this effect. From the preparative vantage point, however, this gap in structural coverage is compensated by chiral rhodium catalysts, which work particularly well with such methyl-capped enyne substrates.[31]

Synthesis of the Antidepressive Agent (−)-GSK 1360707. The excellent results obtained with this set of N-tethered enynes allowed us to apply this chemistry, without amendment, to a highly productive synthesis of GSK 1360707 (**27**). This "triple re-uptake inhibitor" capable of regulating the levels of all three excitatory neurotransmitters (serotonin, noradrenalin, dopamine) in the synaptic clefts is currently in clinical development as a drug candidate for the treatment of severe depression.[32]

It was previously recognized that **27** is poised for noble metal catalysis. Despite an extensive screening campaign, however, the corresponding *N*-nosyl derivative **26** could not be formed with more than 59% ee, using (*R*)-tol-BINAP as the best among all tested ligands (Scheme 5).[33] Therefore, we considered GSK 1360707 a stringent and relevant testing ground for the newly developed gold catalysts presented herein.[34]

Scheme 5. Literature Route to GSK 1360707 (27) by Asymmetric Gold Catalysis[33]

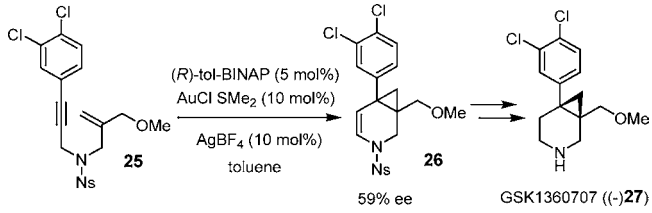

A suitable enyne substrate was prepared in only three high-yielding operations from cheap propargyl amine as shown in Scheme 6. We deliberately replaced the *N*-nosyl substituent chosen by the GSK-team (see compound **25**)[33] by a Cbz

Scheme 6. Enantioselective Synthesis of the Antidepressive Agent GSK 1360707[a]

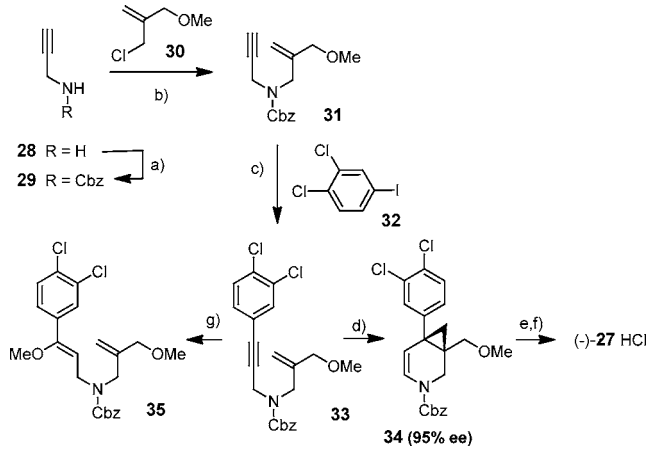

[a]Reagents and conditions: (a) CbzCl, $NaHCO_3$, $EtOH/H_2O$ (1:1), 0 °C → RT, quant.; (b) **30**, NaH, THF/DMF (1:1), 0 °C → RT, 91%; (c) **32**, $[(Ph_3P)_2PdCl_2]$ (2.5 mol %), CuI (5 mol %), Et_3N, DMF, 95%; (d) **15c** (2.75 mol %), $AgBF_4$ (2.5 mol %), toluene, 0 °C, 88% (95% ee); (e) Pd-black (2.5 mol %), H_2 (1 atm), Na_2CO_3, EtOAc/MeOH (1:1), 91%; (f) HCl in ether (1 M), Et_2O, quant.; (g) $[(PhO)_3PAuCl]$ (5.5 mol %), $AgBF_4$ (5 mol %), $MeOH/CH_2Cl_2$ (1:1), 49% (95% brsm).

dx.doi.org/10.1021/ja303641p | J. Am. Chem. Soc. 2012, 134, 15331−15342

group, which promised dividends in the final step of the synthesis. Gratifyingly, exposure of enyne **33** to the cationic gold complex derived from **15c** (2.75 mol %) and $AgBF_4$ (2.5 mol %) in toluene at 0 °C furnished the desired product **34** with an ee of 95% in 88% yield.[35] The exact same ee was obtained with complex **15d**, in which the bis(1-phenethyl)-amine was exchanged for its cyclic congener 2,6-diphenylpiperidine.

This outcome is best appreciated when compared with the results obtained with other gold complexes. Specifically, the analogous phosphoramidite catalyst **10h** incorporating a traditional TADDOL subunit with an annulated isopropylidene acetal gave **34** with only 84% ee (in toluene) or 48% ee (in CH_2Cl_2). This comparison confirms the notion that the acyclic backbone of **15a−d** is in fact an essential design element. Strikingly, the BINOL- or spiro-bisindane derived phosphoramidites **7** and **9** are completely inadequate, furnishing product **34** in ee's as low as 6% and −11%, respectively. Table S-3 contained in the SI provides a more extensive comparison that underpins the superior performance of complexes of type **15** in this particular application.

Stirring of a solution of **34** in EtOAc/MeOH under an atmosphere of hydrogen in the presence of palladium black and Na_2CO_3 led to cleavage of the *N*-Cbz group and saturation of the double bond in a single operation, without any noticeable opening of the cyclopropyl ring or reductive cleavage of the chloride substituents. As a result, the conversion of **34** to **27** is considerably more practical and efficient than the elaboration of the corresponding nosyl derivative **26** previously used.[33] Recrystallization of the hydrochloride salt derived from **27** allows trace metal impurities to be removed, as mandatory for a possible use of this compound in clinical trials.

Overall, we conclude that the new route to GSK 1360707 (**27**) is unprecedentedly short and remarkably productive (five operations, 69% overall yield), because of the unique efficiency of the new gold complex **15c**. It favorably compares with all previous syntheses of this antidepressive agent disclosed in the patent and the open literature.[32,33,36] Moreover, this example shows that asymmetric gold catalysis starts reaching a level of maturity where it becomes relevant for applications in the life sciences.

Oxygen-Tethered Enynes. Oxygen-linked enynes **22** (X = O) are even more demanding substrates than their N-tethered cousins, because they are prone to ether cleavage and/or oligomerization when exposed to Lewis acids. For example, the dinuclear BIPHEP-derived complex **4** with bulky aryl groups on phosphorus usually gave remarkable enantioselectivities but disappointing yields (see Scheme 4).[13] Better results were obtained with chiral rhodium−diene complexes, which were applied, however, only to enynes having *gem*-diphenyl substituents adjacent to the tethering O-atom.[31]

An assortment of substrates with and without such a *gem*-disubstitution pattern were reacted with the new phosphoramidite complexes (Chart 6). The labile product **23j** was obtained in good yield and a respectable ee of 83%; the enantioselectivity was further increased to 93% by incorporation of a *gem*-diphenyl motif next to the O-atom (**23k**). Even better results were obtained for the tricyclic scaffolds **23*l*−p**, which were formed with outstanding optical purity. In the case of product **23p**, the absolute configuration could be unequivocally determined by X-ray diffraction (see the SI); all other compounds were assigned by analogy. As in the N-tethered series, however, this excellent outcome was *contingent upon the presence of an aryl substituent on the alkyne group* (R^3 = aryl); the corresponding substrate with a methyl-capped alkyne furnished product **23q** with only 34% ee. This striking influence is relevant for the interpretation of how the new phosphoramidite ligands might operate and will be addressed in more detail in the computational section of this paper.[37]

Chart 6. Asymmetric Gold-Catalyzed Cycloisomerizations of O-Tethered Enynes[a]

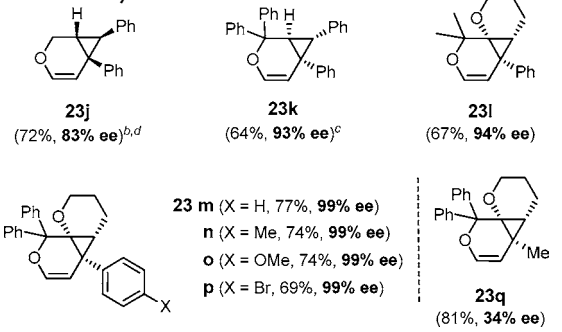

[a]All reactions were performed with (*R,R,R,R*)-**15a** (5.5 mol %), $AgNTf_2$ (5 mol %) in toluene at RT, unless stated otherwise. [b]At −20 °C. [c]At 0 °C. [d]Using complex (*S,S,S,S*)-**15c**.

Furthermore, a pronounced solvent effect on the course of the reaction was noticed (Scheme 7, Table 1). In toluene, compound **23** was formed from **22** as the only observable product (100% by NMR, 99% ee by HPLC). In more polar solvents, however, variable amounts of an isomer were obtained, the unusual constitution of which became clear only after crystals suitable for X-ray diffraction could be grown from **43p** (Ar = *p*-Br-C_6H_4−). In methanol, yet another pathway was dominant, the outcome of which was again ascertained by the crystal structure analysis of product **39p** (see the SI).

Although quite different in structural terms, all three products are thought to derive from a common intermediate (Scheme 7). Thus, activation of the alkyne unit by the gold template engenders the attack of the enol ether to form the carbenoid species **36**.[5,38] In an apolar solvent such as toluene, this reactive intermediate undergoes a rapid 1,2-H shift and demetalation to give product **23**, in which all chiral centers are locked (blue path). In contrast, MeOH allows the homoallyl cation resonance form **38** to unravel, which also has an oxocarbenium character. Loss of the allylic proton then leads to **39** and regenerates the catalyst (green path); it is tempting to assume that MeOH assists this pathway by serving as a proton shuttle.[39] In aprotic dipolar media, however, a more involved mechanism becomes competitive (red path): driven by the formation of a highly stabilized tertiary oxocarbenium ion, the cyclopropyl group of intermediate **37** is shuffled to give **40**. A subsequent shift of the flanking ether oxygen and alkylation of the resulting doubly benzylic cation by the aurated cyclopropyl ring in transannular proximity delivers the rather unusual product **43**. Whether this sequence is stepwise or gains some degree of concertedness cannot be finally answered. The fact, however, that **43** was formed in modest and largely variable optical purity, depending on the chosen medium (Table 1), whereas its companion **23** always had an impeccable ee, suggests that non-negligible charge density gets spread over the various positions of the carbon skeleton en route to **43**. This interpretation is in line with the notion that the reactive

dx.doi.org/10.1021/ja303641p | J. Am. Chem. Soc. 2012, 134, 15331−15342

Scheme 7. Cycloisomerization of the O-Tethered Enynes 22m (Ar = Ph) or 22p (Ar = *p*-Br-C_6H_4−) Catalyzed by 15a /$AgNTf_2$ and the Structure of One of the Two Independent Molecules of Product 43p in the Solid State[a]

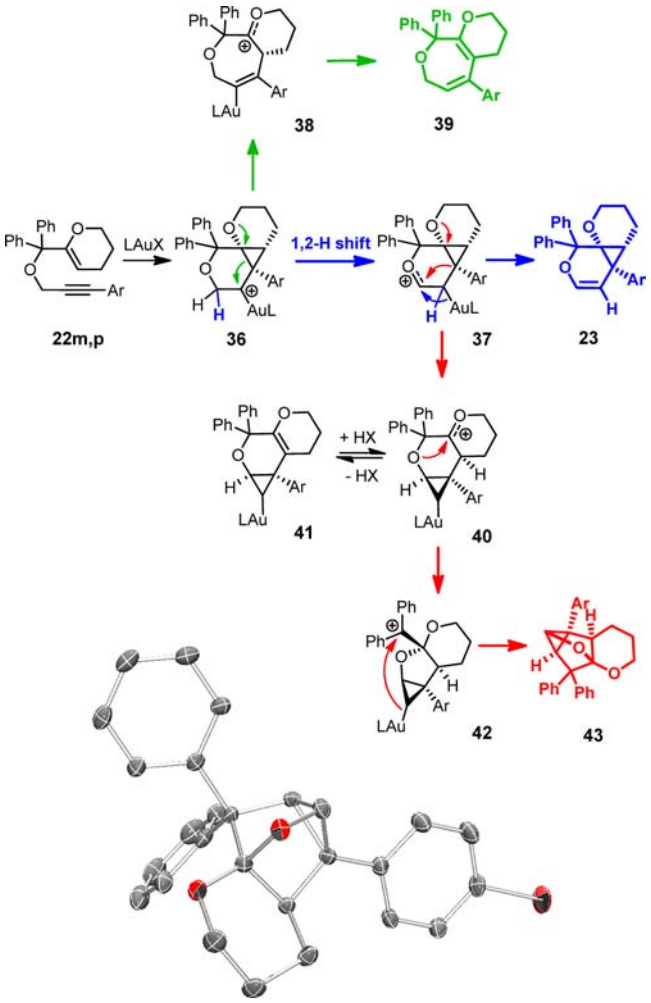

[a]For the full unit cell, see the SI.

Table 1. Solvent Dependence of the Cycloisomerization of Enyne 22m (Ar = Ph) Catalyzed by 15a/$AgNTf_2$

entry	solvent	**23m** (% ee)	**43m** (% ee)	**39m**
1	CH_2Cl_2	74 (99)	26 (48)	
2	acetone	52 (99)	48 (46)	
3	CH_3NO_2	67 (99)	33(52)	
4	THF	66 (99)	24 (4)	10
5	Et_2O	96 (99)	4 (n.d.)[a]	
6	toluene	100 (99)		
7	MeOH			100

[a]n.d. = not determined.

intermediates of noble metal catalyzed enyne cycloisomerizations can exhibit considerable cationic character.[40]

Indoline Formation. The new phosphoramidite ligands also allowed indolines to be accessed in appreciable optical purity from simple substrates (Scheme 8). This transformation is unprecedented and not immediately obvious, since related hydroarylations of allenes catalyzed by carbophilic Lewis acids favored reactions at the distal π-bond.[41−43]

Scheme 8. Asymmetric Gold-Catalyzed Indoline Synthesis[a]

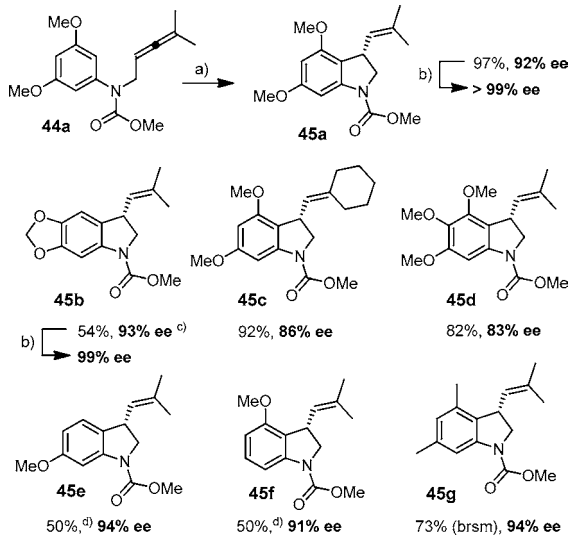

[a]Reagents and conditions: (a) *ent*-**15d** (5.5 mol %), $AgBF_4$ (5 mol %), 1,2-dichloroethane, −30 °C; (b) recrystallization from pentanes; (c) at 0 °C; (d) at −10 °C, 50% (**45e**:**45f** = 28:72).

Treatment of compound **44a** with catalytic amounts of complex **15a** and $AgBF_4$ resulted in near-quantitative hydroarylation of the allene's proximal double bond but a disappointingly low ee (23%). In view of the importance of indolines, however, it was deemed appropriate to optimize this reaction. Taking advantage of the modularity of the ligand architecture and the ease of synthesis, it was swiftly found that complex *ent*-**15d** was uniquely effective (for details, see Table S-4 in the SI). This complex, characterized by a combination of an acyclic dimethyl ether backbone, 2-naphthyl substituents, and a 2,6-diphenylpiperidine moiety, delivered product **45a** with 92% ee; a single recrystallization from pentanes sufficed to give optically pure material.[44] Several other substrates gave similarly respectable results as long as the aromatic moiety to be hydroarylated is electron rich and the N-atom protected as a carbamate; unactivated arenes reacted either very slowly (e.g., formation of **45g**) or even failed to undergo this novel cyclization, whereas substrates endowed with *N*-tosyl groups furnished lower ee's (ca. 60−70%).

Hydroamination and Hydroalkoxylation. The gold-catalyzed intramolecular hydroamination of allenes is another stringent test for the efficacy of the new ligand architecture.[12f,p,45] Gratifyingly, substrates of type **46** were effectively cyclized to the corresponding pyrrolidines **47** with the aid of complex **15b** (Scheme 9), although the ee is responsive to the chosen N-protecting group. Sulfonamides gave good to excellent results (90−95% ee), whereas the corresponding Cbz-derivative **47e** was formed in only low optical purity for reasons that are not entirely clear. Best results were obtained when toluene/EtOAc (1:1) was used as the solvent.[46]

The example shown in Scheme 10 extends this chemistry to an intramolecular hydroalkoxylation, which proceeded with excellent enantioselectivity under the aegis of complex **15c**. Somewhat surprisingly, the best result was obtained in EtOH as the solvent, which did not outperform the attack of the tethered −OH group onto the allene moiety.

Computational Studies. The results summarized above show that the newly designed phosphoramidites comprising a TADDOL-related, yet acyclic backbone are valuable ligands for

dx.doi.org/10.1021/ja303641p | J. Am. Chem. Soc. 2012, 134, 15331−15342

Scheme 9. Asymmetric Gold-Catalyzed Hydroaminations[46,a]

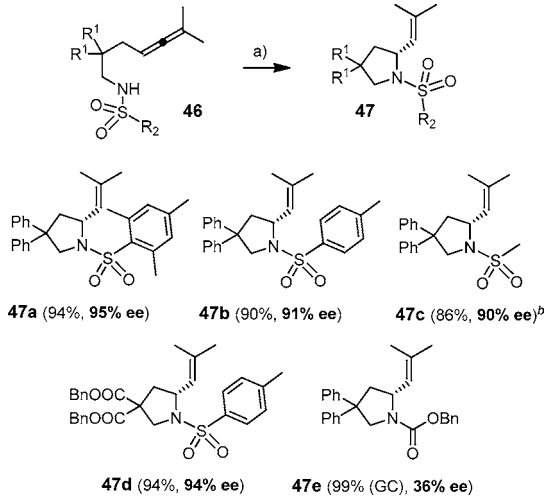

[a]Reagents and conditions: (a) **15b** (5.5 mol %), $AgBF_4$ (5 mol %), toluene/EtOAc (1:1, 0.1 M), 0 °C; (b) at −50 °C.

Scheme 10. Enantioselective Gold-Catalyzed Hydroalkoxylation[46,a]

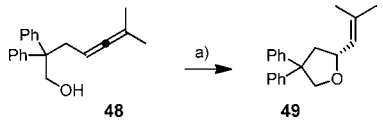

[a]Reagents and conditions: (a) **15c** (5.5 mol %), $AgBF_4$ (5 mol %), EtOH, −60 °C, 93% (96% ee).

a variety of gold-catalyzed cycloaddition, cycloisomerization, and hydroamination/alkoxylation reactions. They are easily prepared on large scale from cheap substrates and amenable to structural editing, and therefore provide opportunities for further fine-tuning. The corresponding gold complexes **15** are air-stable and hence user-friendly tools for organic synthesis.

In view of this favorable profile, a closer look into their mode of action seemed worthwhile. The cycloisomerization of enyne **22h** to **23h** was chosen for this computational study because it proceeds with excellent enantioselectivity and yield alike (94%, 95% ee), and the absolute configuration of **23h** has also been unambiguously determined (see Chart 5 and the SI). Moreover, the crystal structure of precatalyst **15c** (= L*·AuCl in Scheme 11) constitutes a validated starting point (see Figure 2).

On the basis of this solid experimental ground, the cycloisomerization reaction was studied by using density functional theory (DFT). Geometry optimizations were carried out at the BP86/def2-SVP level, with gold being described by an effective core potential (ECP) and the associated def2-ECP basis set. Harmonic force constant calculations were done to characterize the optimized stationary points and to determine the zero-point energy (ZPE) corrections at this DFT level. Free energies were computed by using the rigid-rotor harmonic-oscillator approximation. To check the sensitivity of the computed energy profiles, single-point energies at the optimized BP86/def2-SVP geometries were evaluated by using more advanced functionals (B3LYP, M06), larger basis sets (def2-TZVP, 6-31+G*), dispersion corrections (DFT-D), and solvent corrections (toluene, COSMO). The DFT

Scheme 11. Computed Pathway to (*R*,*R*) Product 23h

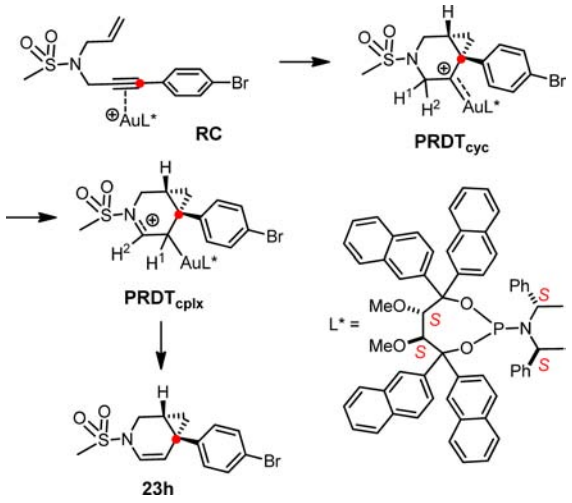

calculations were performed with TURBOMOLE and Gaussian09. The chosen computational procedures and the results obtained are fully specified in the Supporting Information. Here, for the sake of brevity, we only describe the main mechanistic conclusions on the basis of the computed BP86/def2-SVP energy profiles. The higher-level single-point calculations (see above) confirm the qualitative conclusions deduced from the BP86/def2-SVP calculations and generally lead to only rather small changes in the computed energies (see the Supporting Information).

Abstraction of the chloride from **15c** followed by docking of the substrate provides the initial catalyst−substrate complex, in which the effective C_3 symmetry of the precatalyst has given way to a C_1 symmetric environment. This species has a number of low-lying conformers that interconvert via low-barrier internal rotations around single bonds. The starting point for the (*R*,*R*) pathway is a conformer, in which the alkene and alkyne moieties adopt orientations suitable for cyclization. This loaded reactive complex **RC** (Figure 3) lies 3.7 kcal/mol above the most stable catalyst−substrate adduct. As evident from the very uneven Au−C distances (2.18 versus 2.43 Å), this π-complex is highly unsymmetrical, with the metal slipped away

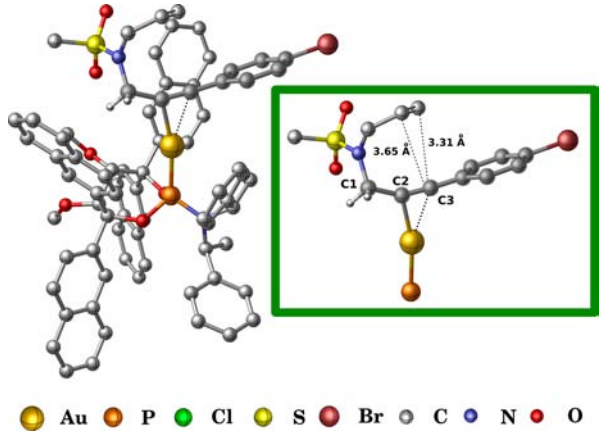

Figure 3. Computed structure of the loaded complex **RC** that serves as entry point to the (*R*,*R*) pathway. Insert: Enlarged view of the reaction center. Bottom: Color code for the elements used in this and the following figures.

dx.doi.org/10.1021/ja303641p | J. Am. Chem. Soc. 2012, 134, 15331−15342

from the arene.[47] The resulting partial positive charge at the benzylic carbon is stabilized by conjugation to the adjacent aromatic π-system. From the stereochemical viewpoint, it is most important to note that the *p*-bromophenyl group on the alkyne lies orthogonal to the naphthyl ring forming the back side of the chiral binding pocket, whereas the ligand's bis(phenethylamine) subunit has turned away at this point.

Rotation of the *N*-allyl subunit over this activated benzylic site leads to the transition state $\mathbf{TS}_{cyc}$, in which the former alkyne clearly deviates from linearity (133.1° for the bond angle $\underline{C}H_2—\underline{C}\equiv\underline{C}—Ar$) (Figure 4). A concerted cyclopropanation

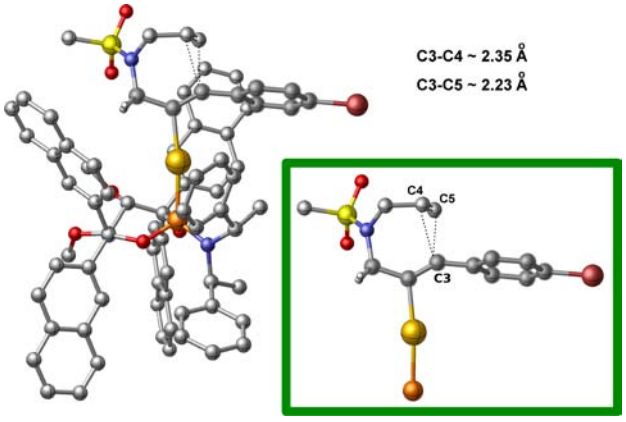

Figure 4. Computed structure of the transition state $\mathbf{TS}_{cyc}$ on the (*R*,*R*) pathway (see caption for Figure 3).

then crafts the cyclic skeleton and delivers the decisive carbenoid complex $\mathbf{PRDT}_{cyc}$ (Figure 5). The two new C−C

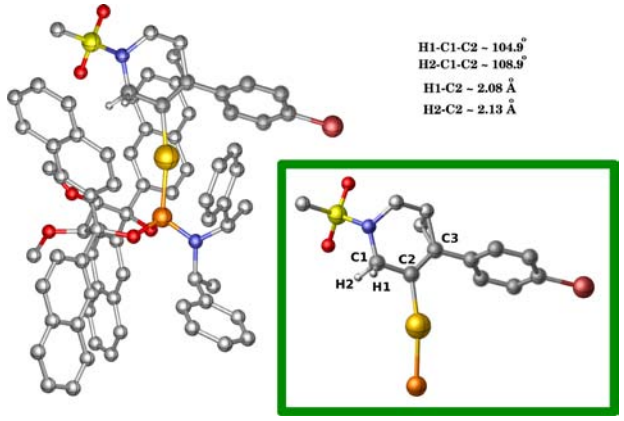

Figure 5. Computed structure of the carbenoid complex $\mathbf{PRDT}_{cyc}$ on the (*R*,*R*) pathway (see caption for Figure 3).

bonds in the cyclopropane ring are formed almost simultaneously, with distances of 2.23 and 2.35 Å at $\mathbf{TS}_{cyc}$.The rehybridization of the former alkyne C-atom (labeled in red in Scheme 11) during this cyclization event enforces a rotatory movement of the aryl group within the chiral cavity. From the projection shown in Figure 4 it is evident that a move to the back would result in a clash with the naphthyl fence. As a consequence, the arene moves to the forefront, while positioning the distinctly smaller incipient cyclopropyl group in the rear. This directionality ultimately results in the formation of the (*R*,*R*)-configured product **23h**, in line with the experimental finding (see Chart 5). The activation barrier of this enantiodetermining step leading from **RC** via $\mathbf{TS}_{cyc}$ to $\mathbf{PRDT}_{cyc}$ is computed to be 9.2 kcal/mol. Figure 6 shows the energy profile of the entire *R*,*R*-selective trajectory in green.

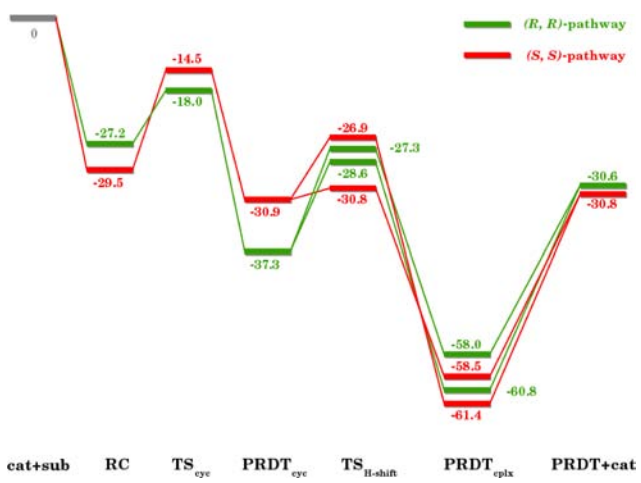

Figure 6. Energy profile (BP86/def2-SVP, kcal/mol) of the enantioselective cycloisomerization of **22h** to **23h** catalyzed by complex **15c**. ZPE corrections are included.

The competing pathway leading to the (*S*,*S*)-enantiomer also deserves comment. In this case, the loaded substrate complex **RC** is actually lower in energy, but the subsequent $\mathbf{TS}_{cyc}$ lies distinctly higher (see the red energy profile in Figure 6). Therefore the selectivity observed in the cycloisomerization of enynes **22** to alkenylcyclopropanes **23** catalyzed by **15c** originates from a Curtin−Hammett situation. The calculated difference between the highest activation barriers of the red and the green channels shown in Figure 6 is 3.5 kcal/mol. All the higher-level single-point energy calculations (see above) confirm that $\mathbf{TS}_{cyc}$ (*S*,*S*) lies above $\mathbf{TS}_{cyc}$ (*R*,*R*), with differences ranging between 1.9 and 4.9 kcal/mol (without ZPE corrections, see the Supporting Information). The formally best gas-phase values with ZPE corrections (B3LYP/def2-TZVP 5.2 kcal/mol; M06/6-31G* 4.0 kcal/mol) are slightly lowered when including dispersion, solvent, and free energy corrections, leading to a best estimate of around 3 kcal/mol. Although this number must not be overinterpreted, it forecasts that the new phosphoramidite ligands impose a significant level of asymmetric induction on the reaction, in accordance with our experimental findings.

Previous labeling studies proved that the evolution of noble-metal carbenoid complexes of type $\mathbf{PRDT}_{cyc}$ to the final product involves a 1,2-H shift.[4c] The current calculations refine this view by showing that the migratory aptitude of the two diastereotopic H-atoms in $\mathbf{PRDT}_{cyc}$ is distinctly different; the energies of the corresponding transition states $\mathbf{TS}_{H\text{-}shift}$ differ by 1.3 kcal/mol in the (*R*,*R*) case (see the Supporting Information). As expected, the adjacent N-atom supports the overall 1,2-H shift by stabilizing the emerging positive charge at its foot. Finally, decomplexation of the resulting intermediate **PRDTcplx** provides the desired product **23h** and regenerates the chiral catalyst L^*Au^+.

As discussed above, one of the naphthyl substituents blocks the back side of the loaded complex **RC** and the transition state $\mathbf{TS}_{cyc}$ in the projections shown in Figures 3 and 4. When the product evolves from there, the orthogonally oriented arene substitutent on the alkyne is forced to rotate to the open

dx.doi.org/10.1021/ja303641p | J. Am. Chem. Soc. 2012, 134, 15331−15342

quadrant in the forefront, while the emerging cyclopropyl ring gets positioned in the crowded rear (Figure 5). Under the proviso that the directionality of this movement is the single most decisive factor for the enantiodetermining step, the striking influence of the nature of the alkyne substituent R^3 on the ee value of the resulting product can be rationalized. It is obvious that the critical size difference between R^3 and the cyclopropyl moiety vanishes for substrates terminated by a methyl group, which in turn explains why the corresponding products **23i** and **23q** were obtained with only modest optical purities.

Conclusions. The outstanding track record of TADDOL in asymmetric synthesis notwithstanding,[23] the opportunities provided by TADDOL-related compounds distinguished by an acyclic backbone were missed prior to our work. Such compounds are valuable building blocks for phosphoramidite ligands, which in turn allow a range of mechanistically distinct gold-catalyzed reactions to be performed with remarkable levels of asymmetric induction; in several cases, optically pure products (≥99% ee) were procured. This outcome is striking if one considers that these ligands can only entertain a one-point binding to the metal. Computational studies provide helpful insights into the origins of enantioselection. In particular they reveal how the effective C_3 symmetry of the gold precatalyst converts into a C_1 symmetric environment upon substrate binding. The latter then translates into the absolute stereochemistry of the product via a previously undescribed unidirectional rotational motion of the reacting centers when passing through the enantiodetermining step. From the practical viewpoint, it is emphasized that the ligand scaffold is readily available and amenable to systematic structural editing. Therefore it is expected that such ligands may find further applications in gold catalysis and beyond.

■ ASSOCIATED CONTENT

Supporting Information

Experimental part: complete ref 32, preparation of substrates, NMR spectra of new compounds, supporting crystallographic information, and additional tables which allow the performance of the new catalysts to be compared in more detail with that of other chiral gold complexes; computational part: computational details, numerical results (relative energies and free energies, NBO charges), plots of all optimized structures, and Cartesian coordinates of all stationary points. This material is available free of charge via the Internet at http://pubs.acs.org.

■ AUTHOR INFORMATION

Corresponding Author

fuerstner@kofo.mpg.de

Notes

The authors declare no competing financial interest.

■ ACKNOWLEDGMENTS

Generous financial support by the MPG, the Fonds der Chemischen Industrie (Kekulé stipend to H.T.) and the Swiss National Science Foundation (stipend to L.M.) is gratefully acknowledged. We thank Dr. S. Flügge and Dr. X. Miao for supportive studies, Mrs R. Leichtweiß for many ee determinations, all analytical departments of our Institute for the excellent support, and Umicore AG & Co KG, Hanau, for a gift of noble metal salts.

■ REFERENCES

(1) (a) Michelet, V.; Toullec, P. Y.; Genêt, J.-P. *Angew. Chem., Int. Ed.* **2008**, *47*, 4268. (b) Aubert, C.; Buisine, O.; Malacria, M. *Chem. Rev.* **2002**, *102*, 813.

(2) (a) Trost, B. M. *Acc. Chem. Res.* **1990**, *23*, 34. (b) Trost, B. M.; Krische, M. J. *Synlett* **1998**, 1.

(3) (a) Chatani, N.; Furukawa, N.; Sakurai, H.; Murai, S. *Organometallics* **1996**, *15*, 901. (b) Blum, J.; Beer-Kraft, H.; Badrieh, Y. *J. Org. Chem.* **1995**, *60*, 5567.

(4) (a) Fürstner, A.; Szillat, H.; Gabor, B.; Mynott, R. *J. Am. Chem. Soc.* **1998**, *120*, 8305. (b) Fürstner, A.; Szillat, H.; Stelzer, F. *J. Am. Chem. Soc.* **2000**, *122*, 6785. (c) Fürstner, A.; Stelzer, F.; Szillat, H. *J. Am. Chem. Soc.* **2001**, *123*, 11863.

(5) (a) Gorin, D. J.; Toste, F. D. *Nature* **2007**, *446*, 395. (b) Fürstner, A.; Davies, P. W. *Angew. Chem., Int. Ed.* **2007**, *46*, 3410. (c) Hashmi, A. S. K. *Chem. Rev.* **2007**, *107*, 3180. (d) Yamamoto, Y. *J. Org. Chem.* **2007**, *72*, 7817. (e) Jiménez-Núñez, E.; Echavarren, A. M. *Chem. Rev.* **2008**, *108*, 3326. (f) Chianese, A. R.; Lee, S. J.; Gagné, M. R. *Angew. Chem., Int. Ed.* **2007**, *46*, 4042. (g) Arcadi, A. *Chem. Rev.* **2008**, *108*, 3266. (h) Li, Z.; Brouwer, C.; He, C. *Chem. Rev.* **2008**, *108*, 3239. (i) Crone, B.; Kirsch, S. F. *Chem.—Eur. J.* **2008**, *14*, 3514. (j) Muzart, J. *Tetrahedron* **2008**, *64*, 5815. (k) Lee, S. I.; Chatani, N. *Chem. Commun.* **2009**, 371. (l) Abu Sohel, S. M.; Liu, R.-S. *Chem. Soc. Rev.* **2009**, *38*, 2269. (m) Nevado, C. *Chimia* **2010**, *64*, 247. (n) Bandini, M. *Chem. Soc. Rev.* **2011**, *40*, 1358. (o) Krause, N.; Winter, C. *Chem. Rev.* **2011**, *111*, 1994.

(6) For pertinent reviews on asymmetric gold catalysis, see: (a) Pradal, A.; Toullec, P. Y.; Michelet, V. *Synthesis* **2011**, 1501. (b) Shapiro, N. D.; Toste, F. D. *Synlett* **2010**, 675. (c) Bongers, N.; Krause, N. *Angew. Chem., Int. Ed.* **2008**, *47*, 2178. (d) Widenhoefer, R. A. *Chem.—Eur. J.* **2008**, *14*, 5382.

(7) The discussion of asymmetric gold catalysis in this paper is limited to examples in which activation of the substrate's π-bond is crucial; other notable but mechanistically different examples of asymmetric gold catalysis include aldol chemistry, asymmetric hydrogenations, dipolar cycloadditions, and the addition of various nucleophiles to carbonyl or carbonyl-derived groups. For leading references, see the following and literature cited therein: (a) Ito, Y.; Sawamura, M.; Hayashi, T. *J. Am. Chem. Soc.* **1986**, *108*, 6405. (b) González-Arellano, C.; Corma, A.; Iglesias, M.; Sánchez, F. *Chem. Commun.* **2005**, 3451. (c) Melhado, A. D.; Amarante, G. W.; Wang, Z. J.; Luparia, M.; Toste, F. D. *J. Am. Chem. Soc.* **2011**, *133*, 3517. (d) Martín-Rodriguez, M.; Nájera, C.; Sansano, J. M.; de Cózar, A.; Cossio, F. P. *Beilstein J. Org. Chem.* **2011**, *7*, 988. (e) Kojima, M.; Mikami, K. *Chem.—Eur. J.* **2011**, *17*, 13950.

(8) (a) For the concept of slippage, see: Eisenstein, O.; Hoffmann, R. *J. Am. Chem. Soc.* **1981**, *103*, 4308. (b) For the isolation of a totally slipped alkene−gold complex, see: Fürstner, A.; Alcarazo, M.; Goddard, R.; Lehmann, C. W. *Angew. Chem., Int. Ed.* **2008**, *47*, 3210.

(9) (a) Hamilton, G. L.; Kang, E. J.; Mba, M.; Toste, F. D. *Science* **2007**, *317*, 496. (b) Aikawa, K.; Kojima, M.; Mikami, K. *Angew. Chem., Int. Ed.* **2009**, *48*, 6073. (c) LaLonde, R. L.; Wang, Z. J.; Mba, M.; Lackner, A. D.; Toste, F. D. *Angew. Chem., Int. Ed.* **2010**, *49*, 598.

(10) For the concept of asymmetric counterion directed catalysis (ACDC), see: Mayer, S.; List, B. *Angew. Chem., Int. Ed.* **2006**, *45*, 4193.

(11) Enantioselective cycloisomerizations of enynes catalyzed by cationic iridium complexes escorted by chiral phosphonates, see: Barbazanges, M.; Augé, M.; Moussa, J.; Amouri, H.; Aubert., C.; Desmarets, C.; Fensterbank, L.; Gandon, V.; Malacria, M.; Ollivier, C. *Chem.—Eur. J.* **2011**, *17*, 13789.

(12) (a) Johansson, M. J.; Gorin, D. J.; Staben, S. T.; Toste, F. D. *J. Am. Chem. Soc.* **2005**, *127*, 18002. (b) Muñoz, M. P.; Adrio, J.; Carretero, J. C.; Echavarren, A. M. *Organometallics* **2005**, *24*, 1293. (c) Tarselli, M. A.; Chianese, A. R.; Lee, S. J.; Gagné, M. R. *Angew. Chem., Int. Ed.* **2007**, *46*, 6670. (d) Liu, C.; Widenhoefer, R. A. *Org. Lett.* **2007**, *9*, 1935. (e) Zhang, Z.; Widenhoefer, R. A. *Angew. Chem., Int. Ed.* **2007**, *46*, 283. (f) LaLonde, R. L.; Sherry, B. D.; Kang, E. J.; Toste, F. D. *J. Am. Chem. Soc.* **2007**, *129*, 2452. (g) Zhang, Z.; Bender,

C. F.; Widenhoefer, R. A. *J. Am. Chem. Soc.* **2007**, *129*, 14148. (h) Melhado, A. D.; Luparia, M.; Toste, F. D. *J. Am. Chem. Soc.* **2007**, *129*, 12638. (i) Watson, I. D. G.; Ritter, S.; Toste, F. D. *J. Am. Chem. Soc.* **2009**, *131*, 2056. (j) Chao, C.-M.; Vitale, M. R.; Toullec, P. Y.; Genêt, J.-P.; Michelet, V. *Chem.—Eur. J.* **2009**, *15*, 1319. (k) Kleinbeck, F.; Toste, F. D. *J. Am. Chem. Soc.* **2009**, *131*, 9178. (l) Kanno, O.; Kuriyama, W.; Wang, Z. J.; Toste, F. D. *Angew. Chem., Int. Ed.* **2011**, *50*, 9919. (m) Cheon, C. H.; Kanno, O.; Toste, F. D. *J. Am. Chem. Soc.* **2011**, *133*, 13248. (n) Corkey, B. K.; Toste, F. D. *J. Am. Chem. Soc.* **2005**, *127*, 17168. (o) Uemura, M.; Watson, I. D. G.; Katsukawa, M.; Toste, F. D. *J. Am. Chem. Soc.* **2009**, *131*, 3464. (p) Zhang, Z.; Bender, C. F.; Widenhoefer, R. A. *Org. Lett.* **2007**, *9*, 2887. (q) Zhang, Z.; Bender, C. F.; Widenhoefer, R. A. *J. Am. Chem. Soc.* **2007**, *129*, 14148. (r) Bandini, M.; Eichholzer, A. *Angew. Chem., Int. Ed.* **2009**, *48*, 9533. (s) Bandini, M.; Monari, M.; Romaniello, A.; Tragni, M. *Chem.—Eur. J.* **2010**, *16*, 14272. (t) Kim, J. H.; Park, S.-W.; Park, S. R.; Lee, S.; Kang, E. J. *Chem. Asian J.* **2011**, *6*, 1982. (u) Wang, M.-Z.; Zhou, C.-Y.; Guo, Z.; Wong, E. L.-M.; Wong, M.-K.; Che, C.-M. *Chem. Asian J.* **2011**, *6*, 812. (v) Brazeau, J.-F.; Zhang, S.; Colomer, I.; Corkey, B. K.; Toste, F. D. *J. Am. Chem. Soc.* **2012**, *134*, 2742. (w) Cera, G.; Chiarucci, M.; Mazzanti, A.; Mancinelli, M.; Bandini, M. *Org. Lett.* **2012**, *14*, 1350. (x) Pradal, A.; Chao, C.-M.; Vitale, M. R.; Toullec, P. Y.; Michelet, V. *Tetrahedron* **2011**, *67*, 4371. (y) Chao, C.-M.; Genin, E.; Toullec, P. Y.; Genet, J.-P.; Michelet, V. *J. Organomet. Chem.* **2009**, *694*, 538. (z) Felix, R. J.; Weber, D.; Gutierrez, O.; Tantillo, D. J.; Gagné, M. R. *Nat. Chem.* **2012**, *4*, 405. (aa) Gawade, S. A.; Bhunia, S.; Liu, R.-S. *Angew. Chem., Int. Ed.* **2012**, *51*, 7835.

(13) (a) Chao, C.-M.; Beltrami, D.; Toullec, P. Y.; Michelet, V. *Chem. Commun.* **2009**, 6988. (b) Pradal, A.; Chao, C.-M.; Toullec, P. Y.; Michelet, V. *Beilstein J. Org. Chem* **2011**, *7*, 1021.

(14) Schmidbaur, H.; Schier, A. *Chem. Soc. Rev.* **2012**, *41*, 370.

(15) (a) Wang, Y.-M.; Kuzniewski, C. N.; Rauniyar, V.; Hoong, C.; Toste, F. D. *J. Am. Chem. Soc.* **2011**, *133*, 12972. (b) Bartolomé, C.; García-Cuadrado, D.; Ramiro, Z.; Espinet, P. *Inorg. Chem.* **2010**, *49*, 9758. (c) For an application in asymmetric gold-catalyzed hydrogenations, see: Arnanz, A.; González-Arellano, C.; Juan, A.; Villaverde, G.; Corma, A.; Iglesias, M.; Sánchez, F. *Chem. Commun.* **2010**, *46*, 3001.

(16) Alonso, I.; Trillo, B.; López, F.; Montserrat, S.; Ujaque, G.; Castedo, L.; Lledós, A.; Mascareñas, J. L. *J. Am. Chem. Soc.* **2009**, *131*, 13020.

(17) Flügge, S., Ph.D. Thesis, Technical University of Dortmund, 2009.

(18) For a preliminary communication, see: Teller, H.; Flügge, S.; Goddard, R.; Fürstner, A. *Angew. Chem., Int. Ed.* **2010**, *49*, 1949.

(19) (a) Gonzáles, A. Z.; Toste, F. D. *Org. Lett.* **2010**, *12*, 200. (b) González, A. Z.; Benitez, D.; Tkatchouk, E.; Goddard, W. A.; Toste, F. D. *J. Am. Chem. Soc.* **2011**, *133*, 5500.

(20) For recent applications of chiral monodentate diaminocarbenes in asymmetric gold catalysis, see: (a) Handa, S.; Slaughter, L. M. *Angew. Chem., Int. Ed.* **2012**, *51*, 2912. (b) Matsumoto, Y.; Selim, K. B.; Nakanishi, H.; Yamada, K.; Yamamoto, Y.; Tomioka, K. *Tetrahedron Lett.* **2010**, *51*, 404. (c) Wang, W.; Yang, J.; Wang, F.; Shi, M. *Organometallics* **2011**, *30*, 3859.

(21) Luzung, M. R.; Mauleón, P.; Toste, F. D. *J. Am. Chem. Soc.* **2007**, *129*, 12402.

(22) Alcarazo, M.; Stork, T.; Anoop, A.; Thiel, W.; Fürstner, A. *Angew. Chem., Int. Ed.* **2010**, *49*, 2542.

(23) For general reviews on TADDOL's and their use in asymmetric synthesis, see: (a) Seebach, D.; Beck, A. K.; Heckel, A. *Angew. Chem., Int. Ed.* **2001**, *40*, 92. (b) Pellissier, H. *Tetrahedron* **2008**, *64*, 10279.

(24) For leading reviews on phosphoramidites and related ligands, see: (a) Teichert, J. F.; Feringa, B. L. *Angew. Chem., Int. Ed.* **2010**, *49*, 2486. (b) Minnaard, A. J.; Feringa, B. L.; Lefort, L.; de Vries, J. G. *Acc. Chem. Res.* **2007**, *40*, 1267. (c) Reetz, M. T. *Angew. Chem., Int. Ed.* **2008**, *47*, 2556.

(25) For a review on TADDOL-derived phosphoramidites and related ligands, see: Lam, H. W. *Synthesis* **2011**, 2011.

(26) Recently, a conceptually different approach to asymmetric gold catalysis using ligands with effective C_3 symmetry has been disclosed, which uses trinuclear gold tris-phospholane complexes: Rodriguez, L.-I.; Roth, T.; Lloret Fillol, J.; Wadepohl, H.; Gade, L. H. *Chem.—Eur. J.* **2012**, *18*, 3721.

(27) (a) An application of a TADDOL with a bis-acetate backbone in a modified Sharpless protocol was largely unsuccessful, cf.: Kanger, T.; Kriis, K.; Paju, A.; Pehk, T.; Lopp, M. *Tetrahedron: Asymmetry* **1998**, *9*, 4475. (b) For studies on the inclusion and host properties of such compounds, see: Toda, F.; Tanaka, K.; Stein, Z.; Goldberg, I. *J. Chem. Soc., Perkin Trans. 2* **1993**, 2359. (c) Toda, F.; Tanaka, K. *Tetrahedron Lett.* **1988**, *29*, 551.

(28) For the interaction between Au^+ and arene rings, see: (a) Xu, F.-B.; Li, Q.-S.; Wu, L.-Z.; Leng, X.-B.; Li, Z.-C.; Zeng, X.-S.; Chow, Y. L.; Zhang, Z.-Z. *Organometallics* **2003**, *22*, 633. (b) Li, Q.-S.; Wan, C.-Q.; Zou, R.-Y.; Xu, F.-B.; Song, H.-B.; Wan, X.-J.; Zhang, Z.-Z. *Inorg. Chem.* **2006**, *45*, 1888. (c) Herrero-Gómez, E.; Nieto-Oberhuber, C.; López, S.; Benet-Buchholz, J.; Echavarren, A. M. *Angew. Chem., Int. Ed.* **2006**, *45*, 5455. (d) Lavallo, V.; Frey, G. D.; Kousar, S.; Donnadieu, B.; Bertrand, G. *Proc. Natl. Acad. Sci. U.S.A.* **2007**, *104*, 13569.

(29) Complexes [**6**·AuCl] and **15b** both furnish the depicted (+)-isomer, the absolute configuration of which was previously determined by Mascareñas, cf. ref 16.

(30) (a) Brissy, D.; Skander, M.; Jullien, H.; Retailleau, P.; Marinetti, A. *Org. Lett.* **2009**, *11*, 2137. (b) Jullien, H.; Brissy, D.; Sylvain, R.; Retailleau, P.; Naubron, J.-V.; Gladiali, S.; Marinetti, A. *Adv. Synth. Catal.* **2011**, *353*, 1109. (c) Brissy, D.; Skander, M.; Retailleau, P.; Frison, G.; Marinetti, A. *Organometallics* **2009**, *28*, 140.

(31) (a) Nishimura, T.; Kawamoto, T.; Nagaosa, M.; Kumamoto, H.; Hayashi, T. *Angew. Chem., Int. Ed.* **2010**, *49*, 1638. (b) Nishimura, T.; Maeda, Y.; Hayashi, T. *Org. Lett.* **2011**, *13*, 3674.

(32) Micheli, F.; et al. *J. Med. Chem.* **2010**, *53*, 4989.

(33) Deschamps, N. M.; Elitzin, V. I.; Liu, B.; Mitchell, M. B.; Sharp, M. J.; Tabet, E. A. *J. Org. Chem.* **2011**, *76*, 712.

(34) For a communication, see: Teller, H.; Fürstner, A. *Chem.—Eur. J.* **2011**, *17*, 7764.

(35) When the reaction was performed in MeOH/CH_2Cl_2 (1:1) with [$(PhO)_3PAuCl$] (5.5 mol%) and $AgBF_4$ (5 mol%), the sensitive enol ether **35** was formed in 49%. The constitution of this product has been erroneously assigned in our original communication as a cyclic ether (compound **15** in ref 34).

(36) (a) Bertani, B.; Di Fabio, R.; Micheli, F.; Tedesco, G.; Terreni S. (Glaxo Group Limited, UK), PCT Int. Appl. WO 2008031772 A1, 2008. (b) Elitzin, V. I.; Harvey, K. A.; Kim, H.; Salmons, M.; Sharp, M. J.; Tabet, E. A.; Toczko, M. A. *Org. Process Res. Dev.* **2010**, *14*, 912.

(37) A substrate with a terminal alkyne afforded an achiral product in high yield, cf.

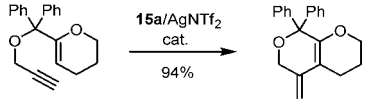

(38) Fürstner, A. *Chem. Soc. Rev.* **2009**, *38*, 3208.

(39) Alternatively, MeOH could intercept the oxocarbenium center, followed by elimination of the resulting glycoside.

(40) (a) Fürstner, A.; Morency, L. *Angew. Chem., Int. Ed.* **2008**, *47*, 5030. (b) Seidel, G.; Mynott, R.; Fürstner, A. *Angew. Chem., Int. Ed.* **2009**, *48*, 2510.

(41) Mamane, V.; Hannen, P.; Fürstner, A. *Chem.—Eur. J.* **2004**, *10*, 4556.

(42) Watanabe, T.; Oishi, S.; Fujii, N.; Ohno, H. *Org. Lett.* **2007**, *9*, 4821.

(43) For other types of gold-catalyzed asymmetric hydroarylation reactions of allenes, see refs 12d and 12e and literature cited therein.

(44) The absolute configuration of **45a** was determined as (*S*) by X-ray diffraction of a derivative, in which the *N*-COOMe group was replaced by a *N*-(3,5-dinitrobenzoate) unit (see the SI).

(45) For related gold-catalyzed hydroaminations of alkenes, see the following for leading references and literature cited therein:

(a) Bender, C. F.; Widenhoefer, R. A. *Org. Lett.* **2006**, *8*, 5303. (b) Zhang, Z.; Lee, S. D.; Widenhoefer, R. A. *J. Am. Chem. Soc.* **2009**, *131*, 5372.

(46) The absolute configuration of compound **47b** [(91% ee) $[\alpha]^{20}_{D}$ +24.9 (*c* 1.0, $CHCl_3$)] was assigned as (*R*) by comparison with literature data for the *S*-enantiomer, which was reported to show an $[\alpha]^{20}_{D}$ −29 (*c* 2.0, $CHCl_3$), cf. ref 12f. The configuration of all other compounds of this series was made by analogy; likewise, the (*R*)-configuration of **49** was confirmed by comparison with literature data of the enantiomer, see: (a) Aikawa, K.; Kojima, M.; Mikami, K. *Adv. Synth. Catal.* **2010**, *352*, 3131; Correction: (b) *Adv. Synth. Catal.* **2011**, *353*, 2875.

(47) In contrast, the known isolated alkyne−gold complexes are largely symmetrical, cf.: (a) Schmidbaur, H.; Schier, A. *Organometallics* **2010**, *29*, 2. (b) Flügge, S.; Anoop, A.; Goddard, R.; Thiel, W.; Fürstner, A. *Chem.—Eur. J.* **2009**, *15*, 8558 and literature cited therein.